Research Square

Preprints are preliminary reports that have not undergone peer review.
They should not be considered conclusive, used to inform clinical practice,
or referenced by the media as validated information.

Discrete Noether Quasi-Symmetries of Non-shifted Generalized Birkhoffian Systems on Time Scales

Xue Tian
Anhui University of Science and Technology
Kuan Yang
Anhui University of Science and Technology
Yi Zhang
zhy@mail.usts.edu.cn

Suzhou University of Science and Technology

Research Article

Keywords: Time scale, Non-shifted system, Generalized Birkhoffian system, Noether quasi-symmetry, Discrete conservation law

Posted Date: November 20th, 2026

DOI: https://doi.org/10.21203/rs.3.rs-11665290/v1

License: This work is licensed under a Creative Commons Attribution 4.0 International License.
Read Full License

Additional Declarations: No competing interests reported.

Discrete Noether Quasi-Symmetries of Non-shifted Generalized Birkhoffian Systems on Time Scales

Abstract

This study investigates generalized Noether quasi-symmetries and the associated conservation laws for non-shifted generalized Birkhoffian systems on time scales. A discrete Pfaff action and a generalized Pfaff–Birkhoff principle are formulated, from which the discrete equations of motion are derived by exploiting the arbitrariness of interior variations. Infinitesimal transformations of time and the Birkhoffian variables are introduced to establish a determining criterion for generalized Noether quasi-symmetry and the corresponding discrete Noether theorem. The derivation explicitly accounts for generalized-force contributions, graininess and jump operators. Two examples illustrate the determination of infinitesimal generators and gauge functions and the construction of the associated conserved quantities. Numerical simulations on fixed-step, variable-step and piecewise-step time scales show that these quantities are preserved up to floating-point round-off errors. For the tested configurations in the second example, the nonuniform meshes yield smaller overall state errors at the same number of steps, whereas the uniform mesh has the shortest measured CPU time. These results clarify the connection between generalized Noether quasi-symmetries and discrete conservation laws and illustrate the importance of assessing state accuracy and computational cost alongside discrete conservation.

Keywords: Time scale, Non-shifted system, Generalized Birkhoffian system, Noether quasi-symmetry, Discrete conservation law

1 Introduction

Time-scale calculus, introduced by Hilger and further developed by Bohner and other researchers [1–3], provides a unified framework for continuous and discrete analysis. This framework allows differential and difference equations to be studied on general time domains [4–10]. Within this framework, early Noether symmetry and conservation laws on time scales were established by Bartosiewicz and Torres [11], and Martins and Torres [12] developed related results using Caputo's duality principle. Since then, Noether symmetries and conservation laws on time scales have attracted considerable research attention, and Noether-type theorems have been established for Hamiltonian systems [13], nonholonomic systems [14], Herglotz-type nonconservative systems [15–17], and Birkhoffian systems [18, 19].

Birkhoffian systems represent a natural generalization of Hamiltonian systems, providing a unified framework for describing both conservative and nonconservative systems, including holonomic and nonholonomic systems. Building on this framework, generalized Birkhoffian systems (GBS) further extend classical Birkhoffian systems by incorporating additional differentiable functions into the equations of motion. These functions appear as generalized-force terms in the corresponding variational principle. Noether symmetries and conservation laws have been investigated for GBS on time scales [20] and for fractional GBS [21]. However, the aforementioned studies of Noether symmetries on time scales are based on shifted formulations.

In variational problems on time scales, shifted and non-shifted formulations coincide in the continuous setting but generally lead to different discrete equations [22, 23]. Consequently, this distinction must be taken into account when deriving discrete symmetry criteria and conservation laws. Noether theorems for non-shifted Birkhoffian and Hamiltonian systems have been established in [24], while corresponding results for constrained Lagrangian systems have been obtained in [25]. Related investigations have also examined Mei symmetries of non-shifted mechanical and Hamiltonian systems [26, 27].

For non-shifted GBS, Chen and Zhang [28] established generalized variational principles, symmetry conditions, and Noether conserved quantities within a general time-scale framework. However, numerical methods specifically designed for these systems remain relatively unexplored, particularly structure-preserving algorithms for numerically verifying the associated conservation properties. Therefore, the development of structure-preserving algorithms for non-shifted GBS on time scales is of considerable significance. A prerequisite for developing such algorithms is to establish a discrete formulation that properly accounts for the additional generalized-force terms, together with the graininess and jump operators. In particular, their contributions to the discrete variational equations, generalized Noether quasi-symmetry criterion, and corresponding conserved quantities need to be explicitly characterized.

Motivated by these considerations, this paper develops a discrete variational framework for non-shifted GBS on time scales. A discrete Pfaff action and the corresponding generalized Pfaff–Birkhoff principle are formulated to derive the discrete equations of motion. Infinitesimal transformations of time and the Birkhoffian variables are then introduced to establish a determining criterion for generalized Noether quasi-symmetry and the associated discrete Noether theorem. In particular, the generalized-force contributions to the discrete variational equations, the quasi-symmetry criterion and the accumulated term in the conserved quantities are explicitly characterized, together with the effects of graininess and jump operators. Two examples illustrate the determination of infinitesimal generators and gauge functions and the construction of the corresponding discrete conserved quantities. Their numerical preservation is examined on uniform and nonuniform meshes. In the second example, fixed-step, variable-step and piecewise-step computations are performed over the same time interval with identical initial conditions and the same number of steps. Componentwise state errors, the overall state error and measured CPU times are compared to examine the effects of mesh selection on numerical accuracy and computational cost.

2 Non-shifted Generalized Birkhoffian Systems on Time Scales

Throughout this paper, repeated component indices are summed from 1 to $2n$ unless they are free indices of an equation. Superscripts σ and ρ denote composition with the forward and backward jump operators, and Δ and ∇ denote the delta and nabla derivatives. Functions and trajectories are assumed to possess the derivatives used below. In the general time-scale formulation, the trajectories are rd-continuous and delta differentiable, and σ is nabla differentiable on the relevant interior domain. The displayed differential equations hold where their derivatives are defined. For time transformations, R_i, B, Λ_i and the infinitesimal generators are taken as restrictions of continuously differentiable functions on an open neighborhood of the time-state domain, so that partial differentiation with respect to time is well defined. For detailed definitions and properties of time scale theory, see Refs. [3] and [23].

Consider a GBS in the shifted formulation on a time scale, described by $2n$ Birkhoffian variables $a_i(t)$, $i = 1, 2, \ldots, 2n$. Let $B_\sigma(t, a_i^\sigma(t))$ denote the Birkhoffian, $R_{i\sigma}(t, a_j^\sigma(t))$ Birkhoff's functions, and $\Lambda_{i\sigma}(t, a_i^\sigma(t))$ the additional terms in the generalized system. Incorporating these additional terms into the corresponding Birkhoff's equations [18, 29] yields the shifted generalized Birkhoff's equations on time scales:

$$\frac{\partial R_{i\sigma}}{\partial a_j^\sigma} a_i^\Delta - \frac{\partial B_\sigma}{\partial a_j^\sigma} - R_{j\sigma}^\Delta + \Lambda_{j\sigma} = 0, \quad i, j = 1, 2, \cdots, 2n \tag{1}$$

The form of Eq. (1) depends on the underlying time scale. On the continuous time scale $\mathbb{T} = \mathbb{R}$, it reduces to the classical generalized Birkhoff's equations:

$$\frac{\partial R_i}{\partial a_j} \dot{a}_i - \frac{\partial B}{\partial a_j} - \dot{R}_j + \Lambda_j = 0 \tag{2}$$

On the uniform discrete time scale $\mathbb{T} = h\mathbb{Z}$, Eq. (1) takes the form

$$\frac{\partial R_{i\sigma,k}}{\partial a_{j,k+1}} (a_{i,k+1} - a_{i,k}) - h \frac{\partial B_{\sigma,k}}{\partial a_{j,k+1}} - R_{j\sigma,k+1} + R_{j\sigma,k} + h\Lambda_{j\sigma,k} = 0 \tag{3}$$

The discrete equations above differ from the conventional discrete Birkhoff's equations [30]. This difference reflects the distinction between shifted and non-shifted variational formulations, which coincide in the continuous setting but generally yield different equations on discrete time scales. Following the non-shifted framework for GBS on time scales [28], the present study adopts a formulation that recovers the conventional discrete generalized Birkhoff's equations as a special case. This formulation provides the basis for deriving the discrete Noether quasi-symmetry criteria and the associated conservation laws.

The Pfaff action for a non-shifted Birkhoffian system on a time scale is defined by

$$S\left(a_i(\cdot)\right) = \int_a^b \left[R_i\left(t, a_j(t)\right) a_i^\Delta(t) - B\left(t, a_i(t)\right)\right] \Delta t, \quad i, j = 1, 2, \ldots, 2n \tag{4}$$

where $B : \mathbb{T} \times \mathbb{R}^{2n} \to \mathbb{R}$ denotes the Birkhoffian and $R_i : \mathbb{T} \times \mathbb{R}^{2n} \to \mathbb{R}$ are Birkhoff's functions. The generalized Pfaff–Birkhoff principle on time scales [28] takes the form

$$\int_a^b \left[\delta \left(R_i \left(t, a_j(t)\right) a_i^{\Delta}(t) - B\left(t, a_i(t)\right)\right) + \Lambda_i \left(t, a_j(t)\right) \delta a_i\right] \Delta t = 0 \tag{5}$$

where the functions $\Lambda_i : \mathbb{T} \times \mathbb{R}^{2n} \to \mathbb{R}$ represent the additional terms in the non-shifted generalized system. The admissible variations satisfy the commutation relations

$$\delta a_i^{\Delta} = (\delta a_i)^{\Delta}, \quad \delta a_i^{\sigma} = (\delta a_i)^{\sigma} \tag{6}$$

together with the endpoint conditions

$$\delta a_i|_{t=a} = \delta a_i|_{t=b} = 0 \tag{7}$$

Applying this principle with the above commutation relations and endpoint conditions yields the non-shifted generalized Birkhoff's equations on time scales:

$$R_j^{\nabla} = \sigma^{\nabla}(t) \cdot \left[\frac{\partial R_i}{\partial a_j} a_i^{\Delta} - \frac{\partial B}{\partial a_j} + \Lambda_j\right], \quad i, j = 1, 2, \ldots, 2n \tag{8}$$

These equations provide the starting point for the discrete variational formulation and the subsequent analysis of discrete Noether quasi-symmetries and conservation laws.

3 Discrete Generalized Birkhoff's Equations on Time Scales

Let Ω be a differentiable manifold of dimension $2n$. Discretize the time interval $[a, b]$ using the nodes $a = t_0 < t_1 < \cdots < t_N = b$, where $t_{k+1} = t_k + \mu_k$ and $b - a = \sum_{k=0}^{N-1} \mu_k$. Here, $\mu_k = \mu(t_k)$, with $\mu(t) = \sigma(t) - t$ denoting the graininess function, and $\sigma(t)$ and $\rho(t)$ are the forward and backward jump operators, respectively. The discrete Pfaff action is defined by

$$S_D = \sum_{k=0}^{N-1} \mu_k \left(R_{i,k} a_{i,k}^{\Delta} - B_k\right) \tag{9}$$

where $a_{i,k} = a_i(t_k)$, $R_{i,k} = R_i(t_k, a_{j,k})$, $B_k = B(t_k, a_{j,k})$, and $a_{i,k}^{\Delta} = \frac{a_{i,k}^{\sigma} - a_{i,k}}{t_k^{\sigma} - t_k} = \frac{a_{i,k+1} - a_{i,k}}{\mu_k}$.

The corresponding discrete generalized Pfaff–Birkhoff principle takes the form

$$\sum_{k=0}^{N-1} \mu_k \left[\delta \left(R_{i,k} a_{i,k}^{\Delta} - B_k\right) + \Lambda_{i,k} \delta a_{i,k}\right] = 0 \tag{10}$$

The admissible variations satisfy the commutation relation

$$\delta a_i^{\Delta} = (\delta a_i)^{\Delta} \tag{11}$$

and the fixed-endpoint conditions

$$\delta a_i|_{t=a} = \delta a_i|_{t=b} = 0 \tag{12}$$

Expanding the variation in Eq. (10) gives

$$\sum_{k=0}^{N-1} \mu_k \left(\frac{\partial R_{i,k}}{\partial a_{j,k}} a_{i,k}^{\Delta} \delta a_{j,k} + R_{i,k} \delta a_{i,k}^{\Delta} - \frac{\partial B_k}{\partial a_{i,k}} \delta a_{i,k} + \Lambda_{i,k} \delta a_{i,k} \right) = 0 \tag{13}$$

Combining the commutation relation in Eq. (11) with the discrete Leibniz rule [3]

$$(f_k \cdot g_k)^{\Delta} = f_k^{\Delta} \cdot g_k + f_k^{\sigma} \cdot g_k^{\Delta} \tag{14}$$

yields

$$R_{i,k} \delta a_{i,k}^{\Delta} = R_{i,k} (\delta a_{i,k})^{\Delta} = \left(R_{i,k}^{\rho} \delta a_{i,k} \right)^{\Delta} - R_{i,k}^{\rho\Delta} \delta a_{i,k} \tag{15}$$

Applying discrete summation by parts and the endpoint conditions in Eq. (12), we obtain

$$\begin{aligned} \sum_{k=0}^{N-1} \mu_k R_{i,k} \delta a_{i,k}^{\Delta} &= \sum_{k=0}^{N-1} R_{i,k} \left(\delta a_{i,k+1} - \delta a_{i,k} \right) \\ &= R_{i,N-1} \delta a_{i,N} - R_{i,0} \delta a_{i,0} + \sum_{k=1}^{N-1} \left(R_{i,k-1} - R_{i,k} \right) \delta a_{i,k} \\ &= - \sum_{k=1}^{N-1} \mu_k R_{i,k}^{\rho\Delta} \delta a_{i,k} \end{aligned} \tag{16}$$

Substituting Eq. (16) into Eq. (13) and collecting the coefficients of $\delta a_{j,k}$ yields

$$\sum_{k=1}^{N-1} \mu_k \left(\frac{\partial R_{i,k}}{\partial a_{j,k}} a_{i,k}^{\Delta} - R_{j,k}^{\rho\Delta} - \frac{\partial B_k}{\partial a_{j,k}} + \Lambda_{j,k} \right) \delta a_{j,k} = 0 \tag{17}$$

Since the interior variations $\delta a_{j,k}$ are arbitrary, their coefficients must vanish:

$$\mu_k \left(\frac{\partial R_{i,k}}{\partial a_{j,k}} a_{i,k}^{\Delta} - R_{j,k}^{\rho\Delta} - \frac{\partial B_k}{\partial a_{j,k}} + \Lambda_{j,k} \right) = 0 \quad k = 1, \ldots, N-1 \tag{18}$$

Using the definitions of the discrete derivatives, Eq. (18) becomes

$$\frac{\partial R_{i,k}}{\partial a_{j,k}} \left(a_{i,k+1} - a_{i,k} \right) - R_{j,k} + R_{j,k-1} - \mu_k \frac{\partial B_k}{\partial a_{j,k}} + \mu_k \Lambda_{j,k} = 0 \tag{19}$$

For a uniform mesh with $\mu_k = h$, Eq. (19) reduces to

$$\frac{\partial R_{i,k}}{\partial a_{j,k}}\left(a_{i,k+1} - a_{i,k}\right) - R_{j,k} + R_{j,k-1} - h\frac{\partial B_k}{\partial a_{j,k}} + h\Lambda_{j,k} = 0 \tag{20}$$

Furthermore, noting that $R_{j,k-1} = R^{\rho}_{j,k}$, we obtain from the definitions of the delta and nabla derivatives that

$$R^{\rho\Delta}_{j,k} = \frac{R_{j,k} - R_{j,k-1}}{\mu_k} = \frac{R^{\nabla}_{j,k}}{\sigma^{\nabla}_k}, \quad \sigma^{\nabla}_k = \frac{\mu_k}{\mu_{k-1}}, \quad k = 1, \ldots, N-1 \tag{21}$$

Substituting Eq. (21) into Eq. (18) and dividing by μ_k yields the discrete generalized Birkhoff's equations in the non-shifted formulation:

$$\frac{\partial R_{i,k}}{\partial a_{j,k}} a^{\Delta}_{i,k} - \frac{R^{\nabla}_{j,k}}{\sigma^{\nabla}_k} - \frac{\partial B_k}{\partial a_{j,k}} + \Lambda_{j,k} = 0 \tag{22}$$

These equations provide the basis for the subsequent analysis of discrete Noether quasi-symmetries and the associated conservation laws.

4 Discrete Noether Theorem on Time Scales

To study the symmetries of the non-shifted discrete generalized Birkhoff's equations derived above, consider the following infinitesimal transformations (ITs) of the discrete time and Birkhoffian variables:

$$t^*_k = t_k + \tilde{\Delta} t_k \tag{23}$$

$$a^*_{i,k} = a_{i,k} + \tilde{\Delta} a_{i,k} \tag{24}$$

Here, $\tilde{\Delta}$ denotes the total variation. To first order in the parameter ε, these transformations can be expressed in terms of the infinitesimal generators ζ_k and $\xi_{i,k}$ as

$$t^*_k = t_k + \varepsilon\zeta_k(t_k, a_{i,k}) \tag{25}$$

$$a^*_{i,k} = a_{i,k} + \varepsilon\xi_{i,k}(t_k, a_{j,k}) \tag{26}$$

In what follows, the variation of the action is evaluated to first order in ε. Expanding the discrete Pfaff action under these transformations, we have

$$\begin{aligned}
\tilde{\Delta} S_D &= \tilde{\Delta}\left[\sum_{k=0}^{N-1} \mu_k \left(R_{i,k} a^{\Delta}_{i,k} - B_k\right)\right] \\
&= \sum_{k=0}^{N-1}\Big[\tilde{\Delta}\mu_k \left(R_{i,k} a^{\Delta}_{i,k} - B_k\right) \\
&\quad + \mu_k \left(\tilde{\Delta} R_{i,k} a^{\Delta}_{i,k} + R_{i,k}\tilde{\Delta} a^{\Delta}_{i,k} - \tilde{\Delta} B_k\right)\Big]
\end{aligned} \tag{27}$$

Using the definition of the delta derivative and the identity $\mu_k = t_{k+1} - t_k$, we obtain

$$(\tilde{\Delta} t_k)^{\Delta} = \frac{\tilde{\Delta} t_{k+1} - \tilde{\Delta} t_k}{t_{k+1} - t_k} = \frac{\tilde{\Delta} \mu_k}{\mu_k} \tag{28}$$

Thus, the variation in graininess is given by

$$\tilde{\Delta} \mu_k = \mu_k \cdot (\tilde{\Delta} t_k)^{\Delta} \tag{29}$$

Substituting Eq. (29) into Eq. (27) gives

$$\begin{aligned} \tilde{\Delta} S_D = \sum_{k=0}^{N-1} \Big[& \mu_k (\tilde{\Delta} t_k)^{\Delta} \left(R_{i,k} a_{i,k}^{\Delta} - B_k \right) \\ & + \mu_k \left(\tilde{\Delta} R_{i,k} a_{i,k}^{\Delta} + R_{i,k} \tilde{\Delta} a_{i,k}^{\Delta} - \tilde{\Delta} B_k \right) \Big] \\ = \sum_{k=0}^{N-1} \mu_k \Big[& R_{i,k} a_{i,k}^{\Delta} (\tilde{\Delta} t_k)^{\Delta} - B_k (\tilde{\Delta} t_k)^{\Delta} \\ & + \tilde{\Delta} R_{i,k} a_{i,k}^{\Delta} + R_{i,k} \tilde{\Delta} a_{i,k}^{\Delta} - \tilde{\Delta} B_k \Big] \end{aligned} \tag{30}$$

The total variation and delta derivative satisfy the relation [3]

$$(\tilde{\Delta} a_{i,k})^{\Delta} = \tilde{\Delta} a_{i,k}^{\Delta} + a_{i,k}^{\Delta} (\tilde{\Delta} t_k)^{\Delta} \tag{31}$$

Using this relation and the first-order expansions of $R_{i,k}$ and B_k, Eq. (30) can be expressed in terms of $\tilde{\Delta} t_k$ and $\tilde{\Delta} a_{i,k}$ as

$$\begin{aligned} \tilde{\Delta} S_D = \sum_{k=0}^{N-1} \mu_k \Bigg[& \left(\frac{\partial R_{i,k}}{\partial t_k} \tilde{\Delta} t_k + \frac{\partial R_{i,k}}{\partial a_{j,k}} \tilde{\Delta} a_{j,k} \right) a_{i,k}^{\Delta} - B_k (\tilde{\Delta} t_k)^{\Delta} \\ & + R_{i,k} (\tilde{\Delta} a_{i,k})^{\Delta} - \frac{\partial B_k}{\partial t_k} \tilde{\Delta} t_k - \frac{\partial B_k}{\partial a_{i,k}} \tilde{\Delta} a_{i,k} \Bigg] \end{aligned} \tag{32}$$

Finally, substituting $\tilde{\Delta} t_k = \varepsilon \zeta_k$ and $\tilde{\Delta} a_{i,k} = \varepsilon \xi_{i,k}$ into Eq. (32) yields

$$\begin{aligned} \tilde{\Delta} S_D = \sum_{k=0}^{N-1} \mu_k \varepsilon \Bigg[& R_{i,k} \xi_{i,k}^{\Delta} + \left(\frac{\partial R_{i,k}}{\partial t_k} \zeta_k + \frac{\partial R_{i,k}}{\partial a_{j,k}} \xi_{j,k} \right) a_{i,k}^{\Delta} \\ & - B_k \zeta_k^{\Delta} - \frac{\partial B_k}{\partial t_k} \zeta_k - \frac{\partial B_k}{\partial a_{i,k}} \xi_{i,k} \Bigg] \end{aligned} \tag{33}$$

Definition 1 (Noether symmetry) The discrete Pfaff action in Eq. (9) admits a Noether symmetry under the ITs in Eqs. (23) and (24) if its total variation satisfies:

$$\tilde{\Delta} S_D = 0 \tag{34}$$

Definition 2 (Noether quasi-symmetry) The ITs in Eqs. (23) and (24) define a Noether quasi-symmetry if there exists a gauge function $G_k = G_k(t_k, a_{i,k})$ such that the total variation of the discrete Pfaff action satisfies

$$\tilde{\Delta} S_D = -\varepsilon \sum_{k=0}^{N-1} \mu_k G_k^{\Delta} \tag{35}$$

Definition 3 (Generalized Noether quasi-symmetry) The ITs in Eqs. (23) and (24) constitute a generalized Noether quasi-symmetry if, for some gauge function G_k, the variation of the discrete Pfaff action satisfies

$$\tilde{\Delta} S_D = -\sum_{k=0}^{N-1} \mu_k \left(\varepsilon G_k^{\Delta} + \Lambda_{i,k} \delta a_{i,k} \right) \tag{36}$$

Here, $\Lambda_{i,k}$ denotes the generalized-force component at t_k, and $\delta a_{i,k} = \tilde{\Delta} a_{i,k} - a_{i,k}^{\Delta} \tilde{\Delta} t_k$ is the corresponding variation at fixed time.

Criterion 1 (Variational criterion) A sufficient condition for the ITs in Eqs. (23) and (24) to define a generalized Noether quasi-symmetry of the non-shifted GBS is that the following identity holds:

$$\begin{aligned} & R_{i,k} (\tilde{\Delta} a_{i,k})^{\Delta} + \left(\frac{\partial R_{i,k}}{\partial t_k} \tilde{\Delta} t_k + \frac{\partial R_{i,k}}{\partial a_{j,k}} \tilde{\Delta} a_{j,k} \right) a_{i,k}^{\Delta} - B_k (\tilde{\Delta} t_k)^{\Delta} \\ & - \frac{\partial B_k}{\partial t_k} \tilde{\Delta} t_k - \frac{\partial B_k}{\partial a_{i,k}} \tilde{\Delta} a_{i,k} + \varepsilon G_k^{\Delta} + \Lambda_{i,k} \left(\tilde{\Delta} a_{i,k} - a_{i,k}^{\Delta} \tilde{\Delta} t_k \right) = 0 \end{aligned} \tag{37}$$

Criterion 2 (Infinitesimal criterion) For the generator representation in Eqs. (25) and (26), the sufficient condition in Criterion 1 takes the form

$$\begin{aligned} & R_{i,k} \xi_{i,k}^{\Delta} + \left(\frac{\partial R_{i,k}}{\partial t_k} \zeta_k + \frac{\partial R_{i,k}}{\partial a_{j,k}} \xi_{j,k} \right) a_{i,k}^{\Delta} - B_k \zeta_k^{\Delta} - \frac{\partial B_k}{\partial t_k} \zeta_k \\ & - \frac{\partial B_k}{\partial a_{i,k}} \xi_{i,k} + G_k^{\Delta} + \Lambda_{i,k} \left(\xi_{i,k} - a_{i,k}^{\Delta} \zeta_k \right) = 0 \end{aligned} \tag{38}$$

Thus, generators ζ_k and $\xi_{i,k}$, together with a gauge function G_k, satisfying this identity determine a generalized Noether quasi-symmetry of the non-shifted GBS.

Theorem 1 (Discrete Noether theorem) *Suppose that the ITs in Eqs. (25) and (26) satisfy the generalized Noether quasi-symmetry condition in Eq. (38). Then, along every solution of the discrete equations (22), the following quantity is conserved at the nodes* $t_k = a + \sum_{m=0}^{k-1} \mu_m \in [a, b]$*:*

$$\begin{aligned} I_D = & \sum_{m=1}^{k} \mu_m \left(\frac{\partial R_{i,m}}{\partial t_m} a_{i,m}^{\Delta} - \frac{\partial B_m}{\partial t_m} + \frac{B_m^{\nabla}}{\sigma_m^{\nabla}} - \Lambda_{i,m} a_{i,m}^{\Delta} \right) \zeta_m \\ & + R_{i,k} \xi_{i,k}^{\sigma} - B_k \zeta_k^{\sigma} + G_k^{\sigma} = \text{const.}, \quad k = 0, \ldots, N-1 \end{aligned} \tag{39}$$

The sum in Eq. (39) is understood to be zero when $k = 0$.

Proof Combining the discrete product rule [3] with Eq. (21) yields

$$R_{i,k}\xi_{i,k}^{\Delta} = \left(R_{i,k}^{\rho}\xi_{i,k}\right)^{\Delta} - \frac{R_{i,k}^{\nabla}}{\sigma_k^{\nabla}}\xi_{i,k} \tag{40}$$

Similarly, $B_k\zeta_k^{\Delta} = \left(B_k^{\rho}\zeta_k\right)^{\Delta} - \frac{B_k^{\nabla}}{\sigma_k^{\nabla}}\zeta_k$. Substituting these identities into Eq. (38) yields

$$\begin{aligned}&\left(R_{i,k}^{\rho}\xi_{i,k}\right)^{\Delta} - \frac{R_{j,k}^{\nabla}}{\sigma_k^{\nabla}}\xi_{j,k} + \left(\frac{\partial R_{i,k}}{\partial t_k}\zeta_k + \frac{\partial R_{i,k}}{\partial a_{j,k}}\xi_{j,k}\right)a_{i,k}^{\Delta} - \left(B_k^{\rho}\zeta_k\right)^{\Delta}\\ &\quad + \frac{B_k^{\nabla}}{\sigma_k^{\nabla}}\zeta_k - \frac{\partial B_k}{\partial t_k}\zeta_k - \frac{\partial B_k}{\partial a_{j,k}}\xi_{j,k} + G_k^{\Delta} + \Lambda_{j,k}\xi_{j,k} - \Lambda_{i,k}a_{i,k}^{\Delta}\zeta_k = 0\end{aligned} \tag{41}$$

Collecting the terms involving ζ_k and $\xi_{j,k}$ gives

$$\begin{aligned}&\left(\frac{\partial R_{i,k}}{\partial t_k}a_{i,k}^{\Delta} - \frac{\partial B_k}{\partial t_k} + \frac{B_k^{\nabla}}{\sigma_k^{\nabla}} - \Lambda_{i,k}a_{i,k}^{\Delta}\right)\zeta_k\\ &\quad + \left(\frac{\partial R_{i,k}}{\partial a_{j,k}}a_{i,k}^{\Delta} - \frac{R_{j,k}^{\nabla}}{\sigma_k^{\nabla}} - \frac{\partial B_k}{\partial a_{j,k}} + \Lambda_{j,k}\right)\xi_{j,k}\\ &\quad + \left(R_{i,k}^{\rho}\xi_{i,k} - B_k^{\rho}\zeta_k + G_k\right)^{\Delta} = 0\end{aligned} \tag{42}$$

Along a solution of Eq. (22), the coefficient of $\xi_{j,k}$ vanishes. Consequently, Eq. (42) reduces to

$$\begin{aligned}&\left(\frac{\partial R_{i,k}}{\partial t_k}a_{i,k}^{\Delta} - \frac{\partial B_k}{\partial t_k} + \frac{B_k^{\nabla}}{\sigma_k^{\nabla}} - \Lambda_{i,k}a_{i,k}^{\Delta}\right)\zeta_k\\ &\quad + \left(R_{i,k}^{\rho}\xi_{i,k} - B_k^{\rho}\zeta_k + G_k\right)^{\Delta} = 0, \quad k = 1, \ldots, N-1\end{aligned} \tag{43}$$

Multiplying by the corresponding graininess and summing over $m = 1, \ldots, k$ yields

$$\begin{aligned}&\sum_{m=1}^{k}\Bigg[\mu_m\left(\frac{\partial R_{i,m}}{\partial t_m}a_{i,m}^{\Delta} - \frac{\partial B_m}{\partial t_m} + \frac{B_m^{\nabla}}{\sigma_m^{\nabla}} - \Lambda_{i,m}a_{i,m}^{\Delta}\right)\zeta_m\\ &\quad + \left(R_{i,m}\xi_{i,m}^{\sigma} - B_m\zeta_m^{\sigma} + G_m^{\sigma}\right) - \left(R_{i,m}^{\rho}\xi_{i,m} - B_m^{\rho}\zeta_m + G_m\right)\Bigg] = 0\end{aligned} \tag{44}$$

Using the shift identities, the difference terms telescope, and Eq. (44) becomes

$$\begin{aligned}&R_{i,k}\xi_{i,k}^{\sigma} - R_{i,0}\xi_{i,0}^{\sigma} - B_k\zeta_k^{\sigma} + B_0\zeta_0^{\sigma} + G_k^{\sigma} - G_0^{\sigma}\\ &\quad + \sum_{m=1}^{k}\mu_m\left(\frac{\partial R_{i,m}}{\partial t_m}a_{i,m}^{\Delta} - \frac{\partial B_m}{\partial t_m} + \frac{B_m^{\nabla}}{\sigma_m^{\nabla}} - \Lambda_{i,m}a_{i,m}^{\Delta}\right)\zeta_m = 0\end{aligned} \tag{45}$$

Separating the terms evaluated at the initial node gives

$$\begin{aligned}&\sum_{m=1}^{k}\mu_m\left(\frac{\partial R_{i,m}}{\partial t_m}a_{i,m}^{\Delta} - \frac{\partial B_m}{\partial t_m} + \frac{B_m^{\nabla}}{\sigma_m^{\nabla}} - \Lambda_{i,m}a_{i,m}^{\Delta}\right)\zeta_m\\ &\quad + R_{i,k}\xi_{i,k}^{\sigma} - B_k\zeta_k^{\sigma} + G_k^{\sigma}\\ &= R_{i,0}\xi_{i,0}^{\sigma} - B_0\zeta_0^{\sigma} + G_0^{\sigma} = \text{const.}\end{aligned} \tag{46}$$

The right-hand side is independent of k, establishing the conservation of the quantity in Eq. (39). □

Remark 1 If $\Lambda_i = 0$ for all $i = 1, 2, \ldots, 2n$, the system reduces to an ordinary non-shifted Birkhoffian system and the conserved quantity (39) reduces to

$$I_D = \sum_{m=1}^{k} \mu_m \left(\frac{\partial R_{i,m}}{\partial t_m} a_{i,m}^{\Delta} - \frac{\partial B_m}{\partial t_m} + \frac{B_m^{\nabla}}{\sigma_m^{\nabla}} \right) \zeta_m + R_{i,k} \xi_{i,k}^{\sigma} - B_k \zeta_k^{\sigma} + G_k^{\sigma} = \text{const.} \tag{47}$$

Thus, Theorem 1 recovers the discrete Noether theorem for non-shifted Birkhoffian systems on time scales [23], including its quasi-symmetric form when a gauge term is present.

Remark 2 For $\mathbb{T} = \mathbb{R}$, the jump operators satisfy $\sigma(t) = \rho(t) = t$, the graininess vanishes, and the delta and nabla derivatives become ordinary time derivatives. Consequently, the conserved quantity in (39) becomes

$$I = R_i \xi_i - B\zeta + G = \text{const.} \tag{48}$$

This recovers the Noether conserved quantity for continuous GBS [31] under the corresponding generalized Noether quasi-symmetry condition.

Remark 3 Let $\mathbb{T} = h\mathbb{Z}$ with $h > 0$ and $t_k = t_0 + kh$, where $t_0 \in \mathbb{T}$. Then $\mu_k = h$ and $\sigma_k^{\nabla} = 1$, while the forward shifts are given by $\xi_{i,k}^{\sigma} = \xi_{i,k+1}$, $\zeta_k^{\sigma} = \zeta_{k+1}$ and $G_k^{\sigma} = G_{k+1}$. Using $a_{i,m}^{\Delta} = (a_{i,m+1} - a_{i,m})/h$ and $B_m^{\nabla} = (B_m - B_{m-1})/h$, Eq. (39) becomes

$$I_D = \sum_{m=1}^{k} \left[\left(\frac{\partial R_{i,m}}{\partial t_m} - \Lambda_{i,m} \right) (a_{i,m+1} - a_{i,m}) - h \frac{\partial B_m}{\partial t_m} + B_m - B_{m-1} \right] \zeta_m + R_{i,k} \xi_{i,k+1} - B_k \zeta_{k+1} + G_{k+1} = \text{const.} \tag{49}$$

Therefore, Theorem 1 gives the discrete Noether theorem for non-shifted GBS on a uniform mesh.

5 Examples

Example 1 Consider the non-shifted GBS on time scales

$$\begin{cases} B = \frac{1}{2} a_3^2 + a_2 \\ R_1 = a_3, \quad R_2 = a_4, \quad R_3 = 0, \quad R_4 = 0 \\ \Lambda_1 = 0, \quad \Lambda_2 = 0, \quad \Lambda_3 = 0, \quad \Lambda_4 = -a_4 \end{cases} \tag{50}$$

Evaluating these functions at the discrete nodes gives

$$\begin{cases} B_k = \frac{1}{2} a_{3,k}^2 + a_{2,k} \\ R_{1,k} = a_{3,k}, \quad R_{2,k} = a_{4,k}, \quad R_{3,k} = 0, \quad R_{4,k} = 0 \\ \Lambda_{1,k} = 0, \quad \Lambda_{2,k} = 0, \quad \Lambda_{3,k} = 0, \quad \Lambda_{4,k} = -a_{4,k} \end{cases} \tag{51}$$

Substituting Eq. (51) into Eq. (22) yields the discrete equations of motion

$$\begin{cases} -\dfrac{a_{3,k}^{\nabla}}{\sigma_k^{\nabla}} = 0 \\ -\dfrac{a_{4,k}^{\nabla}}{\sigma_k^{\nabla}} - 1 = 0 \\ a_{1,k}^{\Delta} - a_{3,k} = 0 \\ a_{2,k}^{\Delta} - a_{4,k} = 0 \end{cases} \tag{52}$$

For this system, Criterion 2 gives the generalized Noether quasi-symmetry condition

$$\begin{aligned} &a_{3,k}\xi_{1,k}^{\Delta} + a_{4,k}\xi_{2,k}^{\Delta} + \xi_{3,k}a_{1,k}^{\Delta} + \xi_{4,k}a_{2,k}^{\Delta} - \frac{1}{2}\left(a_{3,k}^2 + 2a_{2,k}\right)\zeta_k^{\Delta} \\ &- \left(\xi_{2,k} + a_{3,k}\xi_{3,k}\right) + G_k^{\Delta} - a_{4,k}\left(\xi_{4,k} - a_{4,k}^{\Delta}\zeta_k\right) = 0 \end{aligned} \tag{53}$$

Along solutions of Eq. (52), $a_{1,k}^{\Delta} = a_{3,k}$ and $a_{2,k}^{\Delta} = a_{4,k}$. Using these relations, Eq. (53) reduces to

$$\begin{aligned} &a_{3,k}\xi_{1,k}^{\Delta} + a_{4,k}\xi_{2,k}^{\Delta} - \frac{1}{2}\left(a_{3,k}^2 + 2a_{2,k}\right)\zeta_k^{\Delta} \\ &- \xi_{2,k} + G_k^{\Delta} + a_{4,k}a_{4,k}^{\Delta}\zeta_k = 0 \end{aligned} \tag{54}$$

To construct the gauge functions on the chosen time scale, introduce $\Phi_k = \Phi(t_k)$ satisfying

$$\Phi^{\Delta}(t_k) = t_k \tag{55}$$

Expressing the gauge functions through Φ_k accounts for the dependence of delta differentiation on the time scale. Three admissible sets of infinitesimal generators and gauge functions are

$$\begin{cases} \zeta_k^{(1)} = 0 \\ \xi_{1,k}^{(1)} = 0, \quad \xi_{2,k}^{(1)} = t_k, \quad \xi_{3,k}^{(1)} = 0, \quad \xi_{4,k}^{(1)} = 1 \\ G_k^{(1)} = -a_{2,k} + \Phi_k \end{cases} \tag{56}$$

$$\begin{cases} \zeta_k^{(2)} = 0 \\ \xi_{1,k}^{(2)} = t_k, \quad \xi_{2,k}^{(2)} = t_k, \quad \xi_{3,k}^{(2)} = 1, \quad \xi_{4,k}^{(2)} = 1 \\ G_k^{(2)} = -a_{1,k} - a_{2,k} + \Phi_k \end{cases} \tag{57}$$

and

$$\begin{cases} \zeta_k^{(3)} = 1 \\ \xi_{1,k}^{(3)} = 0, \quad \xi_{2,k}^{(3)} = -a_{4,k}, \quad \xi_{3,k}^{(3)} = 0, \quad \xi_{4,k}^{(3)} = 1 \\ G_k^{(3)} = -a_{2,k} \end{cases} \tag{58}$$

By Theorem 1, the corresponding discrete conserved quantities are

$$I_k^{(1)} = t_k^{\sigma}a_{4,k} - a_{2,k}^{\sigma} + \Phi_k^{\sigma} = \text{const.} \tag{59}$$

$$I_k^{(2)} = t_k^{\sigma}\left(a_{3,k} + a_{4,k}\right) - a_{1,k}^{\sigma} - a_{2,k}^{\sigma} + \Phi_k^{\sigma} = \text{const.} \tag{60}$$

and

$$I_k^{(3)} = \sum_{m=1}^{k} \mu_m \left(\frac{B_m^{\nabla}}{\sigma_m^{\nabla}} + a_{4,m}a_{4,m}^{\Delta}\right) - a_{4,k}a_{4,k}^{\sigma} - B_k - a_{2,k}^{\sigma} = \text{const.} \tag{61}$$

On the uniform time scale $\mathbb{T} = h\mathbb{N}$, the antiderivative can be chosen as

$$\Phi_k = \frac{1}{2} t_k^{\rho} t_k \tag{62}$$

For the numerical simulations, prescribe the initial values $a_{1,0} = 0.7$, $a_{2,0} = 0.45$, $a_{3,0} = 0.3$, and $a_{4,0} = 2.0$. For fixed-step computation on $\mathbb{T} = h\mathbb{N}$, take $h = 0.1$ and $N = 200$ time steps. The Birkhoffian variables are computed from Eq. (52), and the conserved quantities are evaluated using Eqs. (59), (60) and (61). The results are presented in Fig. 1, where $I_k^{(1)}$, $I_k^{(2)}$ and $I_k^{(3)}$ are denoted by I_1, I_2 and I_3, respectively.

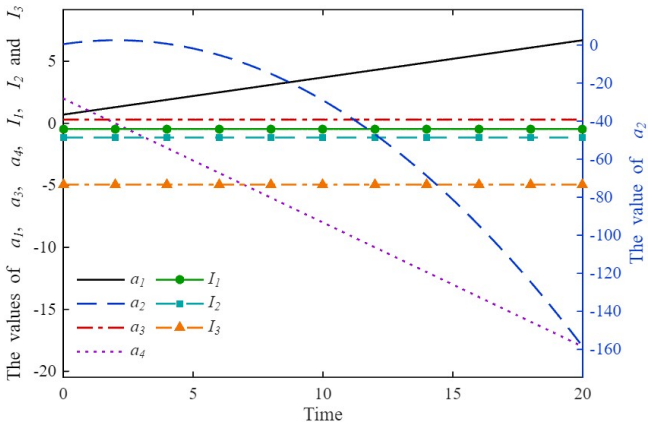

Fig. 1: Birkhoffian variables and conserved quantities on a fixed-step mesh with $h = 0.1$ and $N = 200$

For variable-step computation on the geometric time scale $\mathbb{T} = q^{\mathbb{N}}$ with $q > 1$, the corresponding antiderivative is

$$\Phi_k = \frac{t_k^2}{q+1} \tag{63}$$

The simulation uses $q = 1.02$, $N = 200$ time steps, with the same initial values of the Birkhoffian variables as in the fixed-step case. The results are shown in Fig. 2.

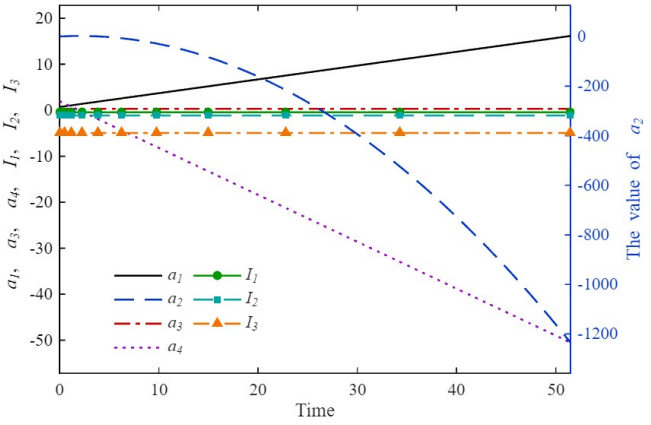

Fig. 2: Birkhoffian variables and conserved quantities on a variable-step mesh with $q = 1.02$ and $N = 200$

To assess the preservation of the three discrete Noether conserved quantities, we evaluate their maximum absolute drifts from the corresponding initial values:

$$E_\ell = \max_{0\le k\le N} \left| I_k^{(\ell)} - I_0^{(\ell)} \right|, \quad \ell = 1, 2, 3$$

Each drift is calculated relative to the initial value on the same time scale. The results for the fixed-step and variable-step meshes are summarized in Table 1.

Table 1: Maximum absolute drifts of the three discrete Noether conserved quantities

Conserved quantity	Fixed-step mesh	Variable-step mesh
I_1	5.2297×10^{-13}	8.6403×10^{-13}
I_2	5.3424×10^{-13}	8.1846×10^{-13}
I_3	4.1922×10^{-13}	3.1797×10^{-13}

All three conserved quantities exhibit maximum absolute drifts below 10^{-12} under both discretizations. These small deviations are consistent with accumulated floating-point round-off and provide numerical evidence for the preservation of the discrete Noether conserved quantities on the tested time scales.

Example 2 Consider a non-autonomous non-shifted GBS with four Birkhoffian variables

$$\begin{cases} B = \dfrac{1}{2}a_3^2 + \dfrac{1}{2}a_4^2, \\ R_1 = ta_3, \quad R_2 = ta_4, \quad R_3 = R_4 = 0, \\ \Lambda_1 = a_3, \quad \Lambda_2 = \Lambda_3 = \Lambda_4 = 0 \end{cases} \tag{64}$$

Evaluating these functions at the discrete nodes gives

$$\begin{cases} B_k = \dfrac{1}{2}a_{3,k}^2 + \dfrac{1}{2}a_{4,k}^2, \\ R_{1,k} = t_k a_{3,k}, \quad R_{2,k} = t_k a_{4,k}, \quad R_{3,k} = R_{4,k} = 0, \\ \Lambda_{1,k} = a_{3,k}, \quad \Lambda_{2,k} = \Lambda_{3,k} = \Lambda_{4,k} = 0 \end{cases} \tag{65}$$

Substitution into Eq. (22) yields the discrete equations of motion

$$\begin{cases} -\dfrac{(t_k a_{3,k})^{\nabla}}{\sigma_k^{\nabla}} + a_{3,k} = 0 \\ -\dfrac{(t_k a_{4,k})^{\nabla}}{\sigma_k^{\nabla}} = 0 \\ t_k a_{1,k}^{\Delta} - a_{3,k} = 0 \\ t_k a_{2,k}^{\Delta} - a_{4,k} = 0 \end{cases} \tag{66}$$

For this system, Criterion 2 takes the form

$$\begin{aligned} & t_k a_{3,k} \xi_{1,k}^{\Delta} + t_k a_{4,k} \xi_{2,k}^{\Delta} + \left(a_{3,k} a_{1,k}^{\Delta} + a_{4,k} a_{2,k}^{\Delta} \right) \zeta_k \\ & - \frac{1}{2} \left(a_{3,k}^2 + a_{4,k}^2 \right) \zeta_k^{\Delta} + G_k^{\Delta} + \left(t_k a_{1,k}^{\Delta} - a_{3,k} \right) \xi_{3,k} \\ & + \left(t_k a_{2,k}^{\Delta} - a_{4,k} \right) \xi_{4,k} + a_{3,k} \left(\xi_{1,k} - a_{1,k}^{\Delta} \zeta_k \right) = 0 \end{aligned} \tag{67}$$

Along solutions of Eq. (66), the coefficients of $\xi_{3,k}$ and $\xi_{4,k}$ vanish. Thus, Eq. (67) reduces to

$$\begin{aligned} & t_k a_{3,k} \xi_{1,k}^{\Delta} + t_k a_{4,k} \xi_{2,k}^{\Delta} + G_k^{\Delta} + a_{3,k} \left(\xi_{1,k} - a_{1,k}^{\Delta} \zeta_k \right) \\ & - \frac{1}{2} \left(a_{3,k}^2 + a_{4,k}^2 \right) \zeta_k^{\Delta} + \left(a_{3,k} a_{1,k}^{\Delta} + a_{4,k} a_{2,k}^{\Delta} \right) \zeta_k = 0 \end{aligned} \tag{68}$$

To construct the generators, introduce a scalar function χ_k on the discrete time scale satisfying

$$\begin{aligned} & t_k \chi_k^{\Delta} + \chi_k = 0, \quad \chi_1 = \frac{1}{t_0}, \\ & \chi_{k+1} = \left(1 - \frac{\mu_k}{t_k} \right) \chi_k, \quad k \geq 1 \end{aligned} \tag{69}$$

Here, $\mu_k = t_{k+1} - t_k$. Assume that $t_k > 0$ and $t_k - \mu_k \neq 0$ at all nodes involved in the construction. The function χ_k depends on the chosen time scale and has the product representation

$$\chi_k = \frac{1}{t_0} \prod_{m=1}^{k-1} \left(1 - \frac{\mu_m}{t_m} \right), \quad k \geq 1 \tag{70}$$

The empty product equals one. To include the initial node in the transformation, set $\chi_0 = 1/(t_0 - \mu_0)$, so that the recurrence in Eq. (69) also holds at $k = 0$. Two sets of infinitesimal generators and gauge functions are

$$\begin{cases} \zeta_k^{(1)} = 0 \\ \xi_{1,k}^{(1)} = \chi_k, \quad \xi_{2,k}^{(1)} = \xi_{3,k}^{(1)} = \xi_{4,k}^{(1)} = 0 \\ G_k^{(1)} = 0 \end{cases} \tag{71}$$

and

$$\begin{cases} \zeta_k^{(2)} = 0 \\ \xi_{1,k}^{(2)} = 0, \quad \xi_{2,k}^{(2)} = 1, \quad \xi_{3,k}^{(2)} = \xi_{4,k}^{(2)} = 0 \\ G_k^{(2)} = 0 \end{cases} \tag{72}$$

Theorem 1 therefore gives the discrete Noether conserved quantities

$$I_k^{(1)} = t_k a_{3,k} \chi_k^{\sigma} = \text{const.} \tag{73}$$

and

$$I_k^{(2)} = t_k a_{4,k} = \text{const.} \tag{74}$$

On the uniform time scale $t_k = t_0 + kh$, with $\mu_k = h$, Eq. (69) gives

$$\chi_k = \frac{1}{t_{k-1}} = \frac{1}{t_k^{\rho}}, \quad k \geq 1 \tag{75}$$

Consequently, the conservation laws become

$$I_k^{(1)} = a_{3,k} = \text{const.}, \quad I_k^{(2)} = t_k a_{4,k} = \text{const.} \tag{76}$$

On the geometric time scale $t_k = t_0 q^k$, with $1 < q < 2$, the graininess is $\mu_k = (q-1)t_k$, and hence

$$\chi_k = \frac{(2-q)^{k-1}}{t_0} \tag{77}$$

The corresponding conserved quantities are

$$I_k^{(1)} = [q(2-q)]^k \, a_{3,k} = \text{const.}, \quad I_k^{(2)} = t_k a_{4,k} = \text{const.} \tag{78}$$

For the numerical simulations, we prescribe the initial conditions $a_{1,0} = 0.5$, $a_{2,0} = 1.0$, $a_{3,0} = 0.3$, and $a_{4,0} = 2.0$ at $t_0 = 0.1$. The initial comparison is performed using $N = 600$ steps over the common interval $[0.1, 6.1]$. Defining the step size as $\mu_k = t_{k+1} - t_k$, we obtain the following update relations from Eq. (66):

$$\begin{cases} a_{1,k+1} = a_{1,k} + \dfrac{\mu_k}{t_k} a_{3,k} \\ a_{2,k+1} = a_{2,k} + \dfrac{\mu_k}{t_k} a_{4,k} \\ a_{3,k+1} = \dfrac{t_k}{t_{k+1} - \mu_{k+1}} a_{3,k} \\ a_{4,k+1} = \dfrac{t_k}{t_{k+1}} a_{4,k} \end{cases} \tag{79}$$

All meshes considered below satisfy $t_k > 0$ and $t_{k+1} - \mu_{k+1} > 0$. As the update for $a_{3,k+1}$ involves μ_{k+1}, one additional mesh node beyond the final time is generated using the same mesh rule.

For the fixed-step simulation, we adopt a uniform mesh $t_k = t_0 + kh$ with $h = 0.01$. The Birkhoffian variables are computed using Eq. (79), while the corresponding conserved quantities are evaluated from Eqs. (73) and (74). The numerical results are presented in Fig. 3. On this uniform mesh, $a_3 = I_k^{(1)}$ holds at each mesh point.

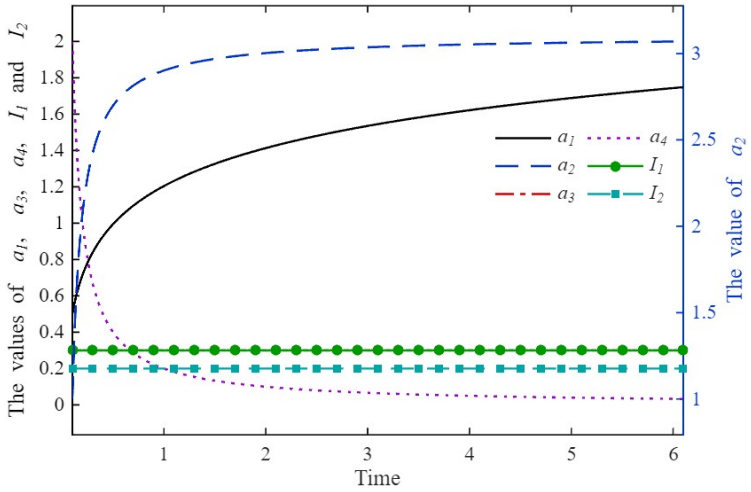

Fig. 3: Birkhoffian variables and conserved quantities on a fixed-step mesh with $h = 0.01$ and $N = 600$

For the variable-step simulation, we adopt the following geometric mesh:

$$t_k = t_0 q^k, \quad q = 61^{1/600}, \quad k = 0, 1, \ldots, 600 \tag{80}$$

This mesh has the same initial and final times and the same number of steps as the uniform mesh. Since $\mu_k = (q-1)t_k$ with $q > 1$, the step size increases monotonically with time. The corresponding numerical results are presented in Fig. 4.

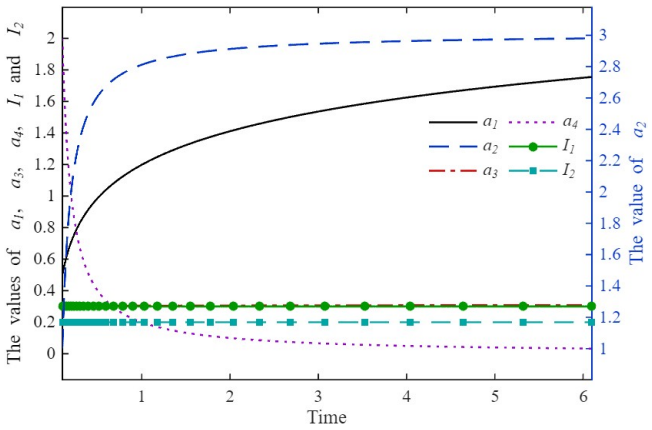

Fig. 4: Birkhoffian variables and conserved quantities on a variable-step mesh with $q = 61^{1/600}$ and $N = 600$

For the piecewise-step simulation, we adopt the following piecewise-uniform mesh:

$$t_k = \begin{cases} 0.1 + 0.002k, & 0 \le k \le 200 \\ 0.5 + 0.008(k-200), & 200 < k \le 400 \\ 2.1 + 0.02(k-400), & 400 < k \le 600 \end{cases} \tag{81}$$

The three subintervals $[0.1, 0.5]$, $[0.5, 2.1]$, and $[2.1, 6.1]$ each contain 200 steps, with corresponding step sizes of 0.002, 0.008, and 0.02, respectively. This mesh provides a finer temporal resolution near the initial time while maintaining the same simulation interval and total number of steps as in the previous two cases. The corresponding numerical results are presented in Fig. 5.

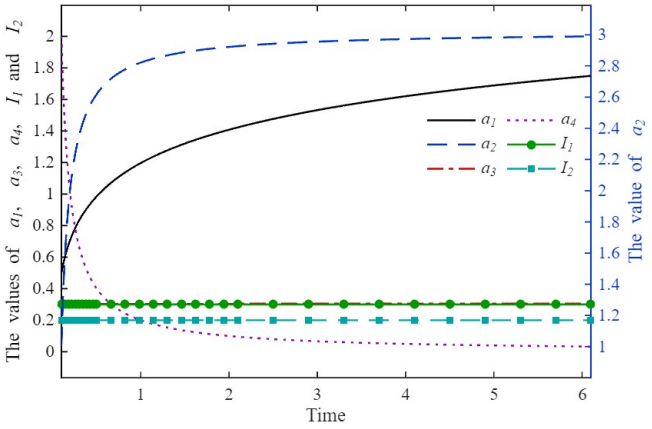

Fig. 5: Birkhoffian variables and conserved quantities on the piecewise-step mesh defined by Eq. (81)

In all three simulations, the conserved quantities remain constant at their initial values, $I_0^{(1)} = 0.3$ and $I_0^{(2)} = 0.2$, up to floating-point roundoff errors. The numerical results presented in Figs. 3, 4 and 5 thus provide numerical evidence for the preservation of the discrete Noether conservation laws on both uniform and nonuniform meshes.

The exact solution of the corresponding continuous system serves as a common reference for evaluating the errors in the state variables:

$$\begin{cases} a_1(t) = 0.5 + 0.3\ln(t/0.1) \\ a_2(t) = 1.0 + 2.0(1 - 0.1/t) \\ a_3(t) = 0.3, \quad a_4(t) = 0.2/t \end{cases} \tag{82}$$

To assess the numerical accuracy, the maximum absolute error for each state component over all computed nodes is defined as

$$E_{a,i} = \max_{0 \le k \le N} |a_{i,k} - a_i(t_k)| \tag{83}$$

The overall state error is then defined as

$$E_a = \max_{1 \le i \le 4} E_{a,i} \tag{84}$$

The update relation for a_4 preserves the invariant $t_k a_{4,k} = t_0 a_{4,0}$ on all three meshes. Consequently, $a_{4,k}$ coincides with the exact continuous solution $a_4(t_k)$ at all computed nodes, up to floating-point roundoff errors. To assess numerical accuracy and computational cost, Table 2 reports the maximum absolute errors in the remaining three state components, the overall state error E_a, and the CPU times for simulations with $N = 600$ steps over the common interval $[0.1, 6.1]$.

CPU time is measured using `cputime` and represents the time required for a single complete computation. The timed operations include mesh generation, array allocation, state updates and their associated denominator checks, and evaluation of the two conserved quantities. Plotting, error evaluation, and file output are excluded. Following warm-up and calibration, each reported CPU time is obtained as the median of five batch-average times, with each batch average calculated by dividing the total batch time by the number of repeated computations.

Table 2: Maximum absolute state errors at the computed nodes for $N = 600$

Time scale	$E_{a,1}$	$E_{a,2}$	$E_{a,3}$	E_a	CPU time (ms)
Fixed-step	0.0150	0.1033	0.0000	0.1033	0.0054
Variable-step	0.0219	0.0135	0.0086	0.0219	0.0506
Piecewise-step	0.0162	0.0228	0.0054	0.0228	0.0058

For $N = 600$, the uniform mesh yields the smallest errors in a_1 and a_3, whereas the geometric mesh achieves the smallest error in a_2 and the lowest overall state error E_a. The piecewise-uniform mesh produces intermediate errors in all three components, with an overall state error of 0.0228, which is close to the value of 0.0219 obtained using the geometric mesh.

Among the three simulations, the uniform mesh has the lowest measured CPU time. The geometric mesh requires approximately 9.37 times the CPU time of the uniform mesh, whereas the piecewise-uniform mesh incurs a computational cost comparable to that of the uniform mesh. Thus, for the present implementation, the piecewise-uniform mesh achieves an overall state error close to that of the geometric mesh while maintaining a computational cost comparable to that of the uniform mesh. It should be noted that these comparisons are based on the same number of steps. A more comprehensive efficiency assessment at a fixed error tolerance would also need to account for the number of steps required to achieve the prescribed accuracy. These results indicate that, although the same discrete Noether invariants are preserved on all three meshes, the state errors and computational costs depend on the mesh configuration. Therefore, conservation properties, numerical accuracy, and computational efficiency should all be considered when selecting an appropriate time scale.

A fixed-step time scale is suitable when the solution varies at a relatively uniform rate throughout the simulation interval or when equally spaced output is required. Although straightforward to implement, a small step size chosen to resolve rapidly varying stages may result in unnecessary computations during slowly varying periods. A prescribed variable-step time scale allows smaller steps to be assigned to rapidly varying stages and larger steps to slowly varying stages, particularly when changes in the variation rate are known in advance. However, its accuracy may vary across state components, and the prescribed mesh does not provide automatic local error control. A piecewise-uniform time scale is particularly suitable when distinct dynamical stages or prescribed time points can be identified, although its effectiveness depends on the appropriate selection of transition times and step sizes. For the present system, abrupt changes in graininess lead to jumps in the discrete values of a_3, which may be reduced by introducing smaller step-size changes or additional transition segments.

Overall, the results in Table 2 highlight the importance of balancing state accuracy and computational cost when choosing among different time scales.

6 Conclusion

This study establishes a discrete variational framework for non-shifted GBS on time scales. Based on the discrete Pfaff action and the generalized Pfaff–Birkhoff principle, the corresponding discrete equations of motion are derived. By introducing infinitesimal transformations, we formulate a generalized Noether quasi-symmetry criterion and establish the associated discrete Noether theorem. These theoretical results establish a connection between quasi-symmetries and conserved quantities along discrete trajectories while explicitly accounting for the effects of generalized forces, graininess, and jump operators.

Two illustrative examples demonstrate the construction of infinitesimal generators, gauge functions, and corresponding conserved quantities. The computed Noether quantities remain constant up to floating-point roundoff errors on the tested uniform and nonuniform meshes. In the second example, comparisons with the exact solution of the corresponding continuous system reveal that state accuracy depends on both the mesh configuration and the state component considered. The numerical results reveal differences in state accuracy and computational cost among the three mesh configurations, despite their preservation of the same discrete Noether invariants. These findings highlight the importance of considering numerical accuracy and computational efficiency alongside discrete conservation properties when selecting an appropriate time scale.

These results also motivate further investigation into the conservation, geometric, and stability properties of numerical methods for non-shifted GBS. In particular, the incorporation of error estimation and step-size selection strategies may help control accumulated state errors while preserving the associated discrete Noether conservation laws, thereby improving the accuracy, reliability, and computational efficiency of long-time simulations. Future work will focus on developing higher-order structure-preserving algorithms for non-shifted GBS.

References

[1] Hilger S: Analysis on measure chains—a unified approach to continuous and discrete calculus. Results in Mathematics **18**, 18–56 (1990) https://doi.org/10.1007/BF03323153

[2] Hilger S: Differential and difference calculus—unified. Nonlinear Analysis: Theory, Methods & Applications **30**, 2683–2694 (1997) https://doi.org/10.1016/S0362-546X(96)00204-0

[3] Bohner M, Peterson A: Dynamic Equations on Time Scales: An Introduction with Applications. Birkhäuser, Boston, MA (2001)

[4] Almeida R, Torres DFM: Isoperimetric problems on time scales with nabla derivatives. Journal of Vibration and Control **15**, 951–958 (2009) https://doi.org/10.1177/1077546309103268

[5] Malinowska AB, Torres DFM: Necessary and sufficient conditions for local pareto optimality on time scales. Journal of Mathematical Sciences **161**, 803–810 (2009) https://doi.org/10.1007/s10958-009-9601-1

[6] Bohner M: Calculus of variations on time scales. Dynamic Systems & Applications **13**, 339–349 (2004)

[7] Han, ZL, Sun SR: Vibration Theory of Dynamic Equations on Time Scales. Shandong University Press, Shandong (2014)

[8] Atici FM, Biles DC, Lebedinsky A: An application of time scales to economics. Mathematical & Computer Modelling **43**, 718–726 (2006) https://doi.org/10.1016/j.mcm.2005.08.014

[9] Fausett LV, Murty KN: Controllability, observability and realizability criteria on time scale dynamical systems. Nonlinear Studies **11**, 627–638 (2004)

[10] Bartosiewicz Z, Kotta Ü, Pawłuszewicz E: Equivalence of linear control systems on time scales. Proceedings of the Estonian Academy of Sciences. Physics, Mathematics **55**, 43–52 (2006)

[11] Bartosiewicz Z, Torres DFM: Noether's theorem on time scales. Journal of Mathematical Analysis and Applications **342**, 1220–1226 (2008) https://doi.org/10.1016/j.jmaa.2008.01.018

[12] Martins N, Torres DFM: Noether's symmetry theorem for nabla problems of the calculus of variations. Applied Mathematics Letters **23**, 1432–1438 (2010) https://doi.org/10.1016/j.aml.2010.07.013

[13] Song CJ, Zhang Y: Conserved quantities for Hamiltonian systems on time scales. Applied Mathematics and Computation **313**, 24–36 (2017) https://doi.org/10.1016/j.amc.2017.05.074

[14] Jin SX, Zhang Y: Generalized Chaplygin equations for nonholonomic systems on time scales. Chinese Physics B **27**, 020502 (2018) https://doi.org/10.1088/1674-1056/27/2/020502

[15] Tian X, Zhang Y: Herglotz variational principle and its Noether theorem on time scales. Chinese Quarterly of Mechanics **39**, 237–248 (2018)

[16] Tian X, Zhang Y: Noether symmetry and conserved quantity for Hamiltonian system of Herglotz type on time scales. Acta Mechanica **229**, 3601–3611 (2018) https://doi.org/10.1007/s00707-018-2188-1

[17] Tian X, Zhang Y: Time-scales Herglotz type Noether theorem for delta derivatives of Birkhoffian systems. Royal Society Open Science **6**, 191248 (2019) https://doi.org/10.1098/rsos.191248

[18] Song CJ, Zhang Y: Noether theorem for Birkhoffian systems on time scales. Journal of Mathematical Physics **56**, 102701 (2015) https://doi.org/10.1063/1.4932607

[19] Song CJ, Zhang Y: Noether theory for Birkhoffian systems with nabla derivatives. Journal of Nonlinear Sciences and Applications **10**, 2268–2282 (2017) https://doi.org/10.22436/jnsa.010.04.76

[20] Song CJ: Quasi-symmetry and conservation laws of generalized Birkhoffian systems on time scales. Journal of Suzhou University of Science and Technology (Natural Science Edition) **37**, 12–17 (2020)

[21] Zhou Y, Zhang Y: Noether symmetries for fractional generalized Birkhoffian systems in terms of classical and combined Caputo derivatives. Acta Mechanica **231**, 3017–3029 (2020) https://doi.org/10.1007/s00707-020-02690-y

[22] Tian X, Zhang Y: A structure-preserving algorithm for time-scale non-shifted Hamiltonian systems. Theoretical and Applied Mechanics Letters **12**, 100368 (2022) https://doi.org/10.1016/j.taml.2022.100368

[23] Tian X, Yang K, Zhang Y: Time-scale discrete Noether symmetries and structure-preserving algorithms for non-migratory Birkhoffian mechanics. Journal of Computational and Applied Mathematics **489**, 117868 (2027) https://doi.org/10.1016/j.cam.2026.117868

[24] Song CJ, Cheng Y: Noether's theorems for non-shifted dynamic systems on time scales. Applied Mathematics and Computation **374**, 125086 (2020) https://doi.org/10.1016/j.amc.2020.125086

[25] Zhang Y: Non-shifted dynamics of constrained systems on time scales under Lagrange framework and its Noether's theorem. Communications in Nonlinear Science and Numerical Simulation **108**, 106214 (2022) https://doi.org/10.1016/j.cnsns.2021.106214

[26] Zhang Y: Mei's symmetry theorem for time scales non-shifted mechanical systems. Theoretical and Applied Mechanics Letters **11**, 100286 (2021) https://doi.org/10.1016/j.taml.2021.100286

[27] Zhang Y: Mei symmetry and conservation laws for time-scale non-shifted Hamilton equations. Advances in Mathematical Physics **2021**, 7329399 (2021) https://doi.org/10.1155/2021/7329399

[28] Chen JY, Zhang Y: Time-scale version of generalized Birkhoffian mechanics and

its symmetries and conserved quantities of Noether type. Advances in Mathematical Physics **2021**, 9982975 (2021) https://doi.org/10.1155/2021/9982975

[29] Ge WK, Mei FX: Time integral theorem for generalized Birkhoffian systems. Acta Physica Sinica **58**, 699–702 (2009) https://doi.org/10.7498/aps.58.699

[30] Kong XL, Wu HB, Mei FX: Structure-preserving algorithms for Birkhoffian systems. Journal of Geometry and Physics **62**, 1157–1166 (2012) https://doi.org/10.1016/j.geomphys.2011.12.004

[31] Mei FX: Dynamics of Generalized Birkhoffian Systems. Science Press, Beijing (2013)